Regime Transitions of Polymer Crystal Growth Rates: Molecular Simulations and Interpretation beyond Lauritzen-Hoffman Model

Wenbing Hu* and Tao Cai

Department of Polymer Science and Engineering, State Key Laboratory of Coordination Chemistry, School of Chemistry and Chemical Engineering, Nanjing University, Nanjing, 210093, China

Received November 28, 2007; Revised Manuscript Received January 4, 2008

ABSTRACT: We report dynamic Monte Carlo simulations of polymer crystal growth induced by a template layer in the melt and semidilute solutions. The molecular simulations evidenced intrinsic regime transitions in the temperature dependence of crystal growth rates, which have been interpreted on the basis of the Lauritzen−Hoffman model, a specific model among the diverse points of view on the general mechanism of polymer crystallization in the literature. We found that, corresponding to the regime II−III transition, there exists a morphological transition from single to multiple lamellar crystal growth, implying the style of spherulite formation changing from a sequential filling to a completed inner filling at low temperatures. Meanwhile, stem-length distributions in the crystallites also exhibit a shift. Dilution makes more perfect chain-folding upon crystal growth, in accord with experimental observations. However, we could not observe the predicted smooth crystal growth front in regime I. In addition, contradictory to the previous expectation, the probability of adjacent chain folding increases slightly at low temperatures. We proposed a new interpretation of regime transitions on the basis of the *intramolecular-crystal-nucleation* model for a better understanding of both experimental and simulation observations.

I. Introduction

Polymer crystallization is one of the fundamentally important phase transitions in polymer materials. It determines the structure and then the application properties of more than two-third of synthetic polymeric products in the present world. Flexible polymers show a strong habit of chain folding that forms lamellar crystallites upon crystallization, as found dating back to 50 years ago in the observations of polyethylene (PE) single crystals.[1−3]

In experiments, the kinetics of lamellar crystal growth are usually reflected by the radial growth rates of polymer spherulites, which show a strong dependence on the supercooling (ΔT), the overshooting of the crystallization temperature (T) away from the equilibrium melting point (T_m^0). Several book chapters and reviews have well summarized the achievements of our current understanding about the temperature dependence of polymer crystal growth rates,[4−9] which constitute a solid background of our present study.

At high crystallization temperatures with minimal supercoolings, polymer crystal growth is usually dominated by the secondary nucleation on a smooth crystal growth front.[4] This idea was inherited from the classical crystal growth models for small molecules by the well-known Lauritzen−Hoffman (LH or HL) model,[10] which is only one specific model among the diverse models on polymer crystallization in the literature.[7−9] In the microscopic details, the LH model assumes that the secondary crystal nucleation is initiated by placing the first crystalline stem on a smooth crystal growth front, followed with lateral spreading via regular chain folding.[11−13] Therefore, under small supercoolings, the advancing speed of the crystal growth front is controlled by the rate for generating one surface nucleus on a smooth crystal growth front.

With the decrease of crystallization temperatures, the lateral spreading rate becomes relatively slow in comparison with the surface nucleation rate, and thus influences the next event of nucleation on the new substrate, as first considered by Hillig[14] for small molecules and later-on developed into the growth of lamellar crystals by Frank.[15] Sanchez and DiMarzio derived the corresponding nucleation rate for the one-dimensional spreading on the growth front of polymer lamellar crystals.[16] This analysis was immediately adopted into the LH theory by Lauritzen and Hoffman and was termed as regime II,[17,18] in order to be distinguished from the high-temperature region named as regime I. Since the overall width of the growth front can be much larger than the actually occupied width for each event of subsequent crystal nucleation, the situation in regime II is featured as multiple nucleation on the smooth substrate, in contrast to the situation in regime I as single nucleation on the smooth substrate.

With further decrease of crystallization temperatures, the above regime analysis of the crystal growth rates sometimes showed a new temperature region with its slope turning back to regime I, as found in polyoxymethylene (POM)[19] and PE.[20] Being regarded as an extension of regime II, the new region at low temperatures was given the name of regime III by Phillips[21] and then was adopted into the LH theory by Hoffman.[22] In this case, due to the higher frequency of surface nucleation at the lower temperatures, the widths of smooth substrates turn out to be close to the thickness of single stems; therefore, the influence of lateral spreading becomes negligible, and the advancing of the crystal growth front is dominated again by the rate of secondary crystal nucleation. The situation is featured as multiple nucleation on the multilayer substrate, in other words, the kinetic roughening on the crystal growth front.

According to the above regime analysis, the measured linear growth rates of polymer lamellar crystals can be described by the rate equation of classical nucleation theory in three separate regimes of crystallization temperatures (denoted from high to low as I, II, and III), as given by

$$G = G_0 \exp[-U/R/(T - T_\infty)] \exp[-K_g/T/\Delta T] \qquad (1)$$

* Corrersponding author. E-mail address: wbhu@nju.edu.cn.

10.1021/ma702636g CCC: $40.75
Published on Web 02/19/2008

where G_0 is a prefactor of crystal growth rates, U the activation energy for a short-range diffusion across interfaces, R the gas constant, T_∞ the Vogel temperature, and K_g the so-called nucleation constant subject to the change among three regimes with the following ratios: $K_g(I):K_g(II):K_g(III) = 2:1:2$.

Up to now, the regime analysis has been widely applied in the study of crystallization kinetics of polymers. Those ratios for all three regimes can be observed in proper molar-mass fractions of several bulk polymers, such as PE,[23] isotactic polypropylene (iPP),[24] poly(ethylene oxide) (PEO),[25] poly(*p*-phenylene sulfide) (PPS),[26] *cis*-polyisoprene (*cis*-PI),[27] and poly-(3,3-dimethylthietane) (PDMT).[28] There are even much more experimental observations on single regime transitions. Here, we will attempt to make a brief summary on the main properties of regime transitions.

1. Morphological Transitions. For bulk PE, regime I−II transition has been supposed to be associated with the morphological transition from axialites to nonbanded spherulites, and in regime III finely banded spherulites are expected, while high-molecular-weight samples show only irregular spherulites.[10,29] Finely structured spherulites were also found in regime II of poly(L-lactic acid) (PLLA)[30] but also in regime III of POM,[19] PEO,[25] and poly(pivalolactone) (PPVL).[31] For single PE crystals grown from the melt, Toda suggested that regime I−II transition corresponds to the morphological transition from the symmetrical lenticular crystal to the truncated lozenge.[32] However, the lenticular crystals could not be observed in the corresponding regime transition in PE solutions.[33] Since the morphological transition and the regime transition may have different criteria, they are not necessary to occur exactly at the same temperatures.[34] Nevertheless, it is safe to say that, from high to low temperatures, regime transitions join together with the tendency toward a denser branching of the ribbonlike lamellar crystals to form finely structured spherulites.[5]

2. Concentration Effect. In dilute PE solutions with various kinds of solvent, only regime I−II transition has been observed.[33,35] Regime II−III transition occurs in the concentrated and bulk PE.[23] The occurrence of regime III seems to be associated with the relatively slow reptation of polymer chains in the bulk phase.[10]

3. Molecular Weight (MW) Effect. This property has been widely studied, for example, in the bulk PE.[10,23] Very short chains exhibit integer chain folding at small supercoolings.[36−38] With the increase of MW, the supercoolings for regime I−II transition are not sensitive to the middle range of MW.[29] Ultrahigh MW PE shows only regime III behaviors (also called regime III-A[10]).[39] Similarly, with the increase of cross-link densities, the gel PE stays only in regime III, until to a high enough density at which regime II−III transition restores.[40] The reptation model has been introduced into the discussion about the MW dependence of regime behaviors.[41,42]

Although there are so many successful applications of the regime analysis, the suspicions have never been completely eliminated. In eq 1, there are as many as four parameters (U, T_∞, K_g, and T_m^0) required to be specified in a certain range of appropriate values according to their physical backgrounds. Variations in the selection of values for U, T_∞ and T_m^0 may give rise to different results of K_g when they are fitted for the experimental data. The width of a smooth substrate for regime I is also difficult to be precisely specified,[43−45] which has raised arguments[46,47] and even the doubt for the existence of regime I.[48] In addition, some other factors, such as the molecular fractionation,[49] the integer-folding of short-chain polymers,[50,51] and the sequence irregularities along the chains,[52] bring also substantial breaks into the temperature dependence of crystal growth rates. Therefore, the intrinsic regime transitions for the folded-chain crystal growth of flexible polymers call for more general evidence.

Dynamic Monte Carlo (MC) simulations on the basis of a simple lattice polymer model[53] are capable to provide general evidence to the intrinsic crystal-growth behaviors of polymers. For example, simulations of lattice polymers have recently reproduced the phenomenon of molecular segregation on crystal growth.[54] The simple lattice model of polymers offers not only a general implication but also a cheap solution to the simulations. The approach of simple lattice polymers thus contains a much wider time window than those approaches bearing chemical details. For instance, molecular dynamics simulations of polyethylene are accessible to the fast crystallization process in the time window of nanoseconds,[55−57] while dynamic MC simulations of lattice polymers may allow us to measure the linear growth rates of polymer crystals in an extensive temperature range possibly covering over regime transitions.

In this report, we launch dynamic MC simulations to observe crystal growth induced by a template layer in both melt and semidilute solutions. The simulations will reproduce the regime-transition phenomena in the sample systems with proper polymer concentrations. We further make some structural analysis, such as stem-length distributions, probabilities of adjacent chain folding, and crystallinities and coil sizes to those polymers participating in the crystalline phase, in association with the regime transitions. We then put forward a new theoretical interpretation to the observed regime transitions on the basis of the intramolecular-crystal-nucleation model.

The paper is organized as follows. After the introduction, we describe the details of simulation approaches. Then, the simulation results in the melt phase are presented, followed with those results in the solutions. We also make statistical evaluations to chain conformation in the semicrystalline texture. After that, we propose a new interpretation of regime transitions. The paper ends up with some concluding remarks.

II. Simulation Techniques

We put 3840 chains, each chain consecutively occupying 128 lattice sites, in a rectangular box of cubic lattice with the sizes $XYZ = 128 \times 64 \times 64$. The occupation density is 0.9375 to mimic a bulk polymer phase, and the small amount of single vacancy sites can be regarded as the free volume necessary for the mobility of polymers. This chain length is large enough to make heavily multiple chain-folding in the lamellar crystal growth (see the results below), and contains some aspects of chain entanglement in the bulk phase.[58] For the polymer solutions with preset concentrations, the total amount of chains was reduced by removing some polymer chains randomly chosen from the melt phase, and those vacancy sites were presumably occupied by the phantom athermal solvent. In the lattice, polymer chains were performing microrelaxation like this: the randomly chosen monomer jumps into a randomly chosen void neighbor, sometimes with partial sliding diffusion along the chain[59] under periodic boundary conditions; meanwhile, both double occupations and bond crossings are not allowed with regard to the hard-core volume exclusions between polymers.

The melt state was prepared by performing athermal relaxation of preset ordered chains for 10^5 MC cycles (each MC cycle has the number of trial moves equal to the total amount of monomers in the sample system, for instance, 4.9×10^5 trial moves in the bulk phase), while the first eight chains exhibiting

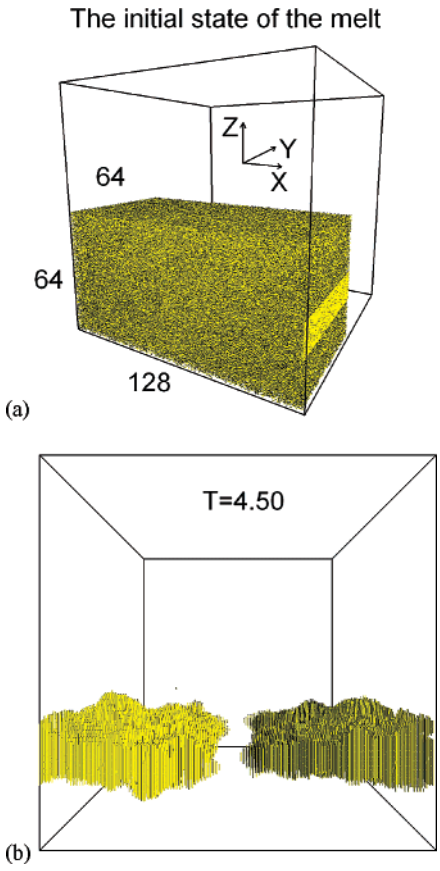

Figure 1. Snapshots of (a) the initial state for crystal growth and (b) the crystal growth state at the temperatures 4.50 after the period of 4.3 $\times$ 10^4 MC cycles for the melt samples containing a template of folded chains with folding lengths 16 at $X = 128$. In part a, all the polymer bonds are drawn in tiny cylinders, and in part b, only the bonds containing more than 15 parallel neighbors (presumably meaning the crystalline bonds) are drawn in tiny cylinders.

uniform fold lengths at 16 and 7 times folding were fixed at the position $X = 128$ for a template layer to induce crystal growth. The snapshot of the melt phase is shown in Figure 1a. Crystal growth will be induced from both sides of the template layer and develops along the long X-axis, as shown in Figure 1b.

In our simulations, the crystallization was mainly driven by the parallel attractions between polymer bonds (denoted as E_p).[53,60] We also charged the potential energy penalty for noncollinear connection of consecutive bonds along the chain (denoted as E_c) and the frictional barrier for crystal thickening via *c*-slip diffusion of the chains in the crystalline phase (denoted as E_f).[61] The mixing interactions between the monomer sites and the solvent sites were set as zero for polymer solutions containing with an athermal solvent. Conventional Metropolis sampling was employed in each trial move with a potential energy barrier $E = (pE_p + cE_c + \Sigma f_i E_f)/kT = (pE_p/E_c + c + \Sigma f_i E_f)E_c/kT$, where p, c, and Σf_i were the net amount of nonparallel pairs of neighboring bonds, the net amount of noncollinear connections of consecutive bonds along the chain, and the sum of parallel neighbors along the path of local sliding diffusion, respectively, and k was the Boltzmann constant. In practice, E_p/E_c was fixed at one to drive the crystallization and meanwhile to keep the chain flexible at crystallization temperatures; and E_f/E_c was fixed at 0.02 to prohibit a large extent of crystal thickening right behind the crystal growth front and thus to secure the heavily multiple chain-folding in the crystal. E_f may provide an additional stability to the crystalline phase and

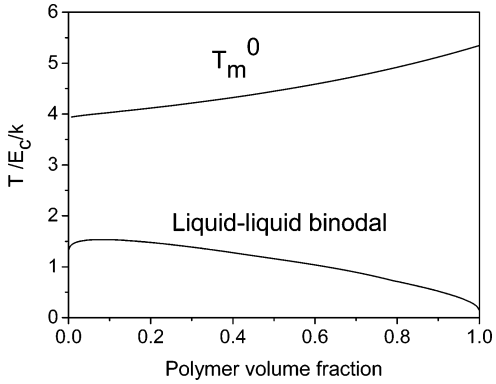

Figure 2. Theoretical phase diagrams of polymer solutions with an athermal solvent and $E_p/E_c = 1$ for lattice polymers with the chain lengths 128, calculated from the developed mean-field lattice theory for polymer solutions.[53]

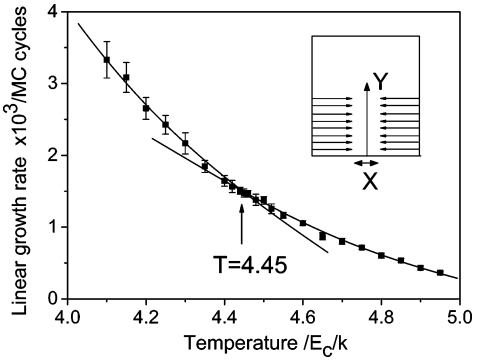

Figure 3. Linear growth rates measured at variable temperatures from the melt phase, demonstrating two regimes of temperature dependences. The curves are drawn to guide the eyes and the arrow indicates the transition temperature at 4.45.

thus shifts the melting point up to some extent. We quenched the initial melt to variable low temperatures by setting the values of kT/E_c (simply denoted as T below), and observed the crystal growth induced by the template layer. A snapshot for lamellar crystal growth initiated from both sides of the template layer in the melt phase is shown in Figure 1b. The crystal thickness is close to that of the template layer, demonstrating heavily multiple chain-folding in the crystal (about seven-times chain-folding for the chain length 128 and the effect of integer folding becomes negligible).

We measured the linear crystal growth rates under variable temperatures. To this end, we averaged over those slopes on the time evolution of the crystal growth front separately obtained at 16 equally spaced Y positions (eight positions on each side of the template, see the inset in Figure 3), provided that the advancing of the crystal growth front exhibits a linear relationship with the time evolution. The crystal growth front on the *X*-axis was registered by the largest distance of consecutively four crystalline bonds away from the template, where each crystalline bond contained more than 15 parallel neighbors along the *Z*-axis. The time windows for the program running in a single PC machine (CPU 2.4 GHz) were set from several hours to several weeks.

Crystallization from the semidilute solutions manifests itself as a condensation process. Therefore, crystal growth will decrease polymer concentration in the amorphous phase of solutions and thus changes the thermodynamic condition for further crystal growth. In reality, however, a large reservoir of solutions with an almost constant polymer concentration is usually present for the growth of single crystals. To mimic such

a situation of reality, we inserted polymer chains away from the crystal growth front to maintain the preset concentration in the amorphous phase of solutions during crystal growth. To this end, we recorded the positions of polymer chains that contain at least one monomer located at the sectional area $X = 64$ in the initial melt. During crystal growth, one chain will be randomly selected from these recorded chains and be inserted into its initial position as soon as the polymer concentration in the amorphous phase becomes lower than the preset value due to crystal growth. Such an insertion process can maintain well the preset concentration in the amorphous phase of semidilute solutions and hence preserves an almost constant thermodynamic condition for crystal growth.

The crystallizability of polymers in an athermal solvent brings a metastable liquid−liquid-phase separation beneath the equilibrium melting point.[62,63] The latter may influence the crystal growth at low temperatures. We, therefore, calculated both liquid−liquid binodal and liquid−solid coexistence curves on the basis of the recently developed mean-field lattice theory[53] for the above polymer solutions. The results are shown in Figure 2. One can see that the metastable liquid−liquid demixing occurs in the region much lower than the temperature window of our observations reported below, and thus it will not influence the studied crystal growth at low temperatures.

In the following, we report first the simulation results obtained from the bulk phase, followed with the results obtained from the solutions, and then we make some structural analysis of chain conformation in the semicrystalline texture. After that, we provide a new interpretation to our observations of regime transitions.

III. Simulation Results and Discussion

A. Crystal Growth from the Melt. Under variable temperatures, the linear growth rates of polymer lamellar crystals in the melt are summarized in Figure 3. Two temperature regimes of crystal growth rates with the transition temperature at $T = 4.45$ can be recognized. The lower temperature regime shows a relatively strong temperature dependence of crystal growth rates, implying the existence of regime III.

We employed the regime analysis by applying eq 1 to calculate the ratio of nucleation constants between two regimes observed in Figure 3. Since the simulations contained no significant activation energy for polymer diffusion in the melt, only the melting point T_m^0 required for specification. We found that if the melting point is deliberately chosen at 5.70, an excellent agreement with the regime II−III transition can be observed, as demonstrated in Figure 4a. Furthermore, under the conditions that the correlation coefficients of linear regression in each regime are higher than 0.99, all the possible melting points give the ratios of nucleation constants near the value of two, as shown in Figure 4b. Note that the above melting points are all slightly higher than the theoretical melting point (5.20) calculated in Figure 2, probably due to the introduction of E_f energy in our simulations. Since traditionally, the supercooling itself can be further calibrated due to the weak temperature dependence of both entropy and heat of fusion,[64,65] in addition, the weak temperature dependences of other factors in eq 1 are usually neglected, the practical ratios of nucleation constants are allowed to deviate slightly away from the precise value of two. Therefore, the results in Figure 4b tell us that in a certain range of melting points a precise selection of the value may not be a vital factor to observe regime II−III transition. The above observations thus evidence the generality of intrinsic regime II−III transition for folded-chain crystal growth of polymers.

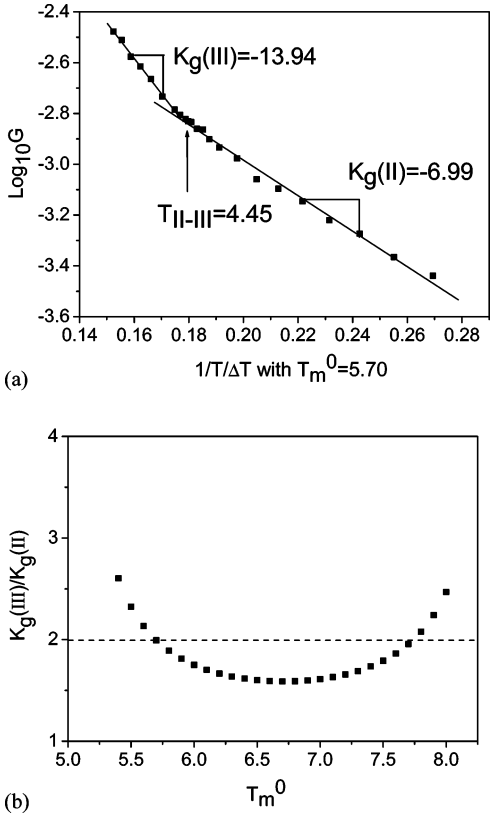

Figure 4. (a) Logarithmic linear growth rates vs $(1/T)/\Delta T$ with $T_m^0 = 5.70$, showing two distinct regimes with the ratio of their slopes close to two for crystal growth from the melt. The straight lines result from linear regression. The arrow indicates the transition temperature at 4.45. (b) Ratios of the nucleation constants between two regimes showing the values around two in a wide range of melting points. The nucleation constants were obtained from the linear regression of the growth rate data in each regime with the correlation coefficient higher than 0.99. The dashed line indicates the values of two.

Visual inspections on the snapshots of crystallites obtained at various temperatures show that with the decrease of temperatures a morphological transition from single lamellar growth to multilamellar growth occurs exactly at $T = 4.45$, as demonstrated in Figure 5a,b in comparison with Figure 1b. One can see from Figure 5a that new lamellar crystals are not initiated by the template layer at the beginning of crystal growth; rather, it is produced by the intrinsic growth instability during crystal growth. At this temperature or even higher, the baby lamella lags behind the parent lamella, characterized in a large-scale morphology as the lamellar branching (meaning side branching). Below this temperature, the baby lamella grows together with the parent lamella and shares the same positions of the growth fronts, as shown in Figure 5b, characterized in a large-scale morphology as the lamellar splaying (meaning top branching). We also provide the corresponding movies of these crystal growth as Supporting Information in the journal website.

Branching and splaying make two different filling styles of spherulite formation at low temperatures, i.e., sequential filling and completed inner filling, respectively.[66] With a sequential filling, the dominant lamellae make first the frame of spherulite and then its inner space is filled by the subsidiary lamellae branching from the dominant lamellae either at lower temperatures or at later periods of crystallization. In contrast, with a completed inner filling, the high splaying rate of crystal growth makes the spherulite immediately filled with lamellae at the crystal growth front. Such a continuous growth in the latter case may endow the spherulite with a banded structure under

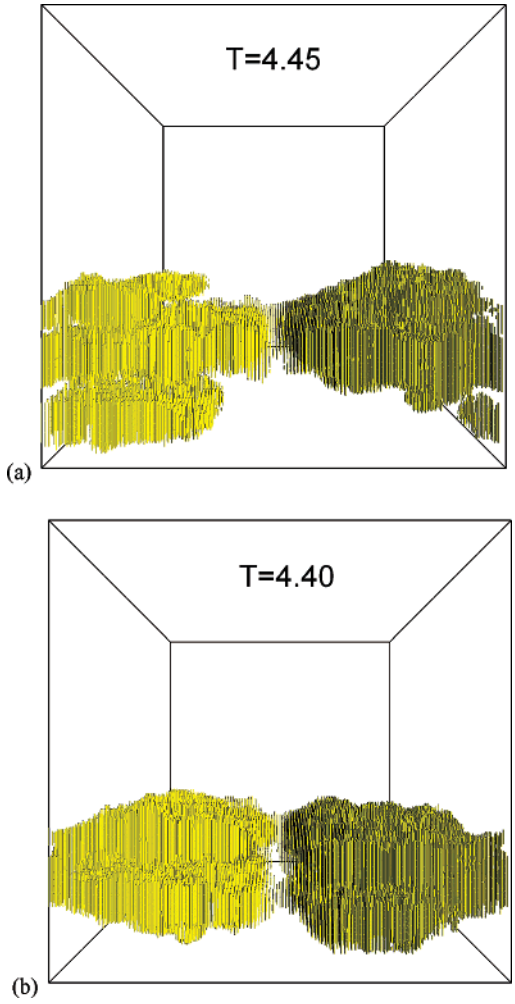

Figure 5. Snapshots of the crystal growth states at the temperatures (a) 4.45 and (b) 4.40 after the periods of 4.3×10^4 and 3.8×10^4 MC cycles respectively for the melt samples containing a template of folded chains with folding lengths 16 at $X = 128$. Only the bonds containing more than 15 parallel neighbors are drawn in tiny cylinders.

polarized optical microscopy.[10,67] Phillips and Vatansever have, indeed, observed that regime II is prone to exhibit abundant lamellar branching on the crystal growth of *cis*-PI, while the branches become probably invisible in regime III with dense splaying upon lamellar growth.[27] Cheng et al. even observed that around regime II−III transition, the spherulite of iPP gradually changes its optical sign from negative to positive under polarized optical microscopy.[24] Such positive spherulites of iPP correspond to the dominant cross-hatched epitaxial branching for a complete filling of spherulites at low temperatures.[68] Cheng et al. also observed the Maltese cross pattern occurring in regime III of PEO, implying well organized lamellar stacking due to splaying growth of lamellar crystals along the radius directions of the spherulites.[25] Therefore, the simulation observations allow us to assign the morphological aspects of lamellar growth in separate regimes to the different filling styles of spherulites in the trend toward finely structured spherulites at lower temperatures.

Crystal thickness is another morphological character being often studied in experiments. The crystal thickness is characterized by the stem lengths in the crystallites. We further checked the stem-length distributions and their mean values in the crystallites obtained from the melt under variable temperatures. The results are reported in Figure 6a,b. One can see a small break in the decaying crystal thickness at regime II−III

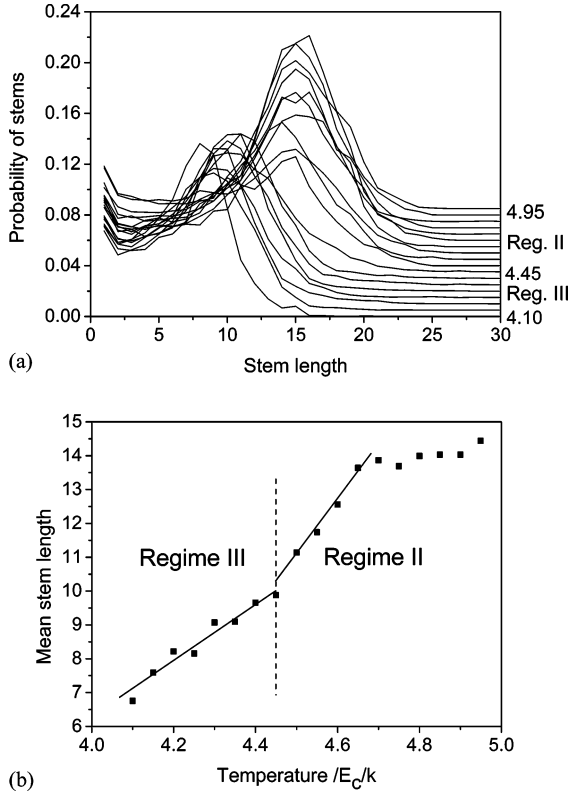

Figure 6. (a) Stem-length distributions and (b) mean stem lengths in the crystallites grown from the melt under variable temperatures. The stem length was defined as the number of consecutively connected crystalline bonds along the chain, each crystalline bond containing more than 15 parallel neighbors. In part a, the curves are drawn with equally spaced vertical offsets for clarity. In part b, the straight lines are drawn to guide the eyes.

transition, the phenomenon never observed before in the experiments probably due to their limited resolution of observations on the molecular-level details. Near the high-temperature end, the mean stem lengths become saturated, probably due to the crystalline phase containing too high frictional barrier for sliding diffusion with E_f energy and even beyond the efficiency of metropolis sampling. It is not surprise to see that before saturation the mean stem lengths exhibit a nearly linear dependence on the reciprocal of supercooling with the equilibrium melting point selected at 5.70. Such a linear relationship with the correlation coefficient higher than 0.99 can be found in a wide range of T_m^0 from 5.3 to 7.4, evidencing the similar experimental observations on the temperature dependence of crystal thickness.[4,5]

The measured crystal thickness is obtained at the later stage of crystal growth after many complicated processes such as instant thickening at the crystal growth front,[69] isothermal thickening inside the crystal, and crystal perfection. Therefore, the topics like the evolutions of crystal thickness and surface free energies from the critical nuclei to the mature crystallites require for further elaborate studies. These topics, although very interesting, have been beyond the scope of our present study.

In regime III, multiple lamellae are generated as shown in Figure 5b. One polymer chain may participate both lamellae upon their parallel growth. To check the probability of such cases, we calculated the vertical outreach of those crystalline bonds in each chain, i.e., the difference between the highest and the lowest *Z*-positions of those bonds containing 15 parallel neighbors in each polymer. The results for the distribution of polymers are reported in Figure 7. One can see that the probabilities for single polymers joining two lamellae (vertical

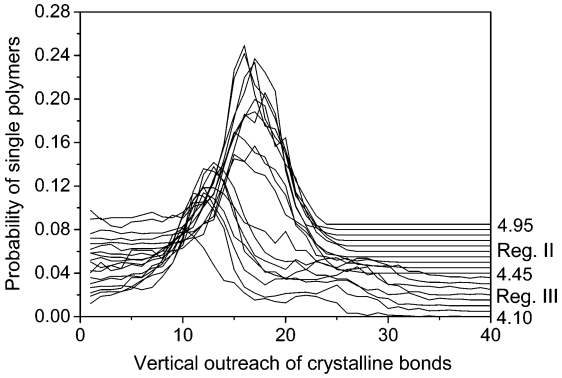

Figure 7. Distributions of the vertical outreaches of crystalline bonds in single polymers after crystal growth in the melt. The crystalline bonds contain more than 15 parallel neighbors. The curves are drawn with equally spaced vertical offsets for clarity.

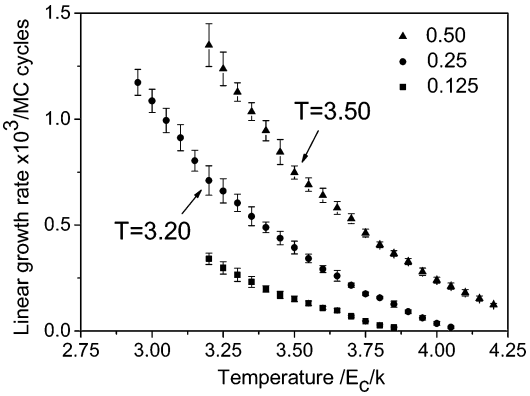

Figure 8. Linear growth rates measured under variable temperatures for polymer solutions with three denoted polymer volume fractions. The arrows indicate the transition temperatures (in units of E_C/k) from single-lamellar to multiple-lamellar growth.

outreach >20) rise in regime III, but not approach the same heights as those peaks standing for single lamella. This is because in the initial melt the mean-square radius of gyration of polymers (128-mers) are measured at about 30, showing the vertical outreach of an average coil at about 11, comparable with the crystal thickness of single lamella but much less than the vertical outreach for double lamellae. Anyway, the parallel growth of two lamellae within a distance comparable with the coil sizes makes not only the tie molecules between them but also the interlocks of their loops (also called as dead entanglements), which will restrict the feeding of polymer chains for lateral spreading at the growth front and thus gives rise to regime III behaviors.

B. Crystal Growth from Solutions. Crystal growth in regime I was extremely slow in the melt phase. This behavior prevented us from observing regime I−II transition in the melt due to the limited time window of our simulations. We therefore made dilution to the bulk phase and reduced the total amount of polymer chains to enhance the computation efficiency in each MC cycle. The linear growth rates of polymer crystals in the solutions with several polymer concentrations are summarized in Figure 8. The arrows in the figure indicate the transitions from single-lamellar to multiple-lamellar growth. In the lowest concentration (polymer volume fraction 0.125), only single-lamellar growth can be observed, implying no regime III in this semidilute solution.

We employed first the regime analysis to the polymer solution with the lowest concentration 0.125. As demonstrated in Figure 9a, the results show two temperature regimes if we select the

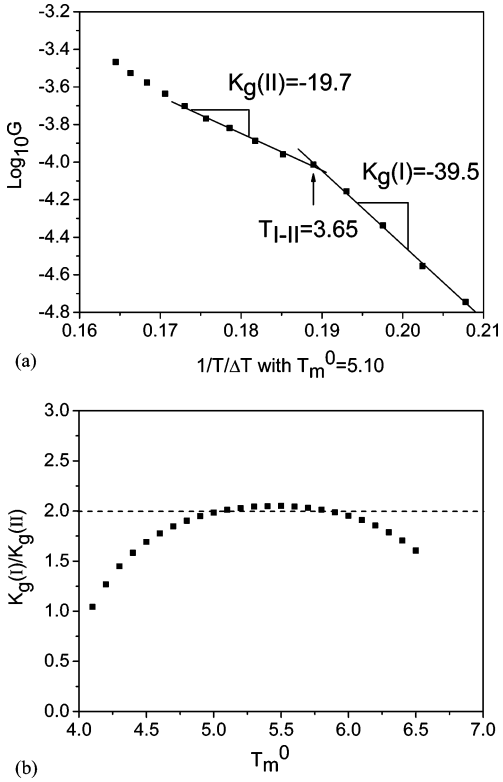

Figure 9. (a) Logarithmic linear growth rates vs $(1/T)/\Delta T$ with $T_m^0 = 5.10$, showing two distinct regimes with the ratio of their slopes close to two in the solution with polymer volume fraction 0.125. The straight lines result from linear regression. The arrow indicates the transition temperature at 3.65. (b) Ratios of the nucleation constants between two regimes showing the values around two in a wide range of melting points. The nucleation constants were obtained from the linear regression of the growth rate data in each regime with the correlation coefficient higher than 0.99. The dashed line indicates the values of two.

melting point at 5.10. The ratio of the nucleation constants of two regimes demonstrates a good regime I−II transition. The data points near the low-temperature end deviate from regime II, but appear to be not the same as for regime III according to their growth morphologies of single lamella and the nucleation constant. We attribute such a deviation from regime II at low temperatures as the influence of polymer diffusion in semidilute solutions to crystal growth, where the inserted chains may directly diffuse toward the fast advancing crystal growth front without making a homogeneous distribution in the amorphous phase of the solution. Below the lower end of temperatures, the constant linear growth rates became unavailable.

We found again that the observations of regime I−II transition are not sensitive to the selection of the melting point in a certain range of temperatures, as demonstrated in Figure 9b. Note that this range is still higher than the theoretical prediction of the equilibrium melting point (4.05) calculated in Figure 2, and this difference can be attributed to E_f energy in the crystalline phase. The above observations thus evidence the generality of intrinsic regime I−II transition for folded-chain crystal growth of polymers.

Around regime I−II transition shown in Figure 9a, the stem-length distributions in the crystallites shift down continuously with the decrease of temperatures, as shown in Figure 10. It is again no surprise to see the linear dependence of mean stem lengths on the reciprocal supercoolings with the melting point selected at 5.10. We found that all the melting points selected in a wide range from 4.50 to 6.50 give the correlation coefficients of linear regression higher than 0.99, evidencing

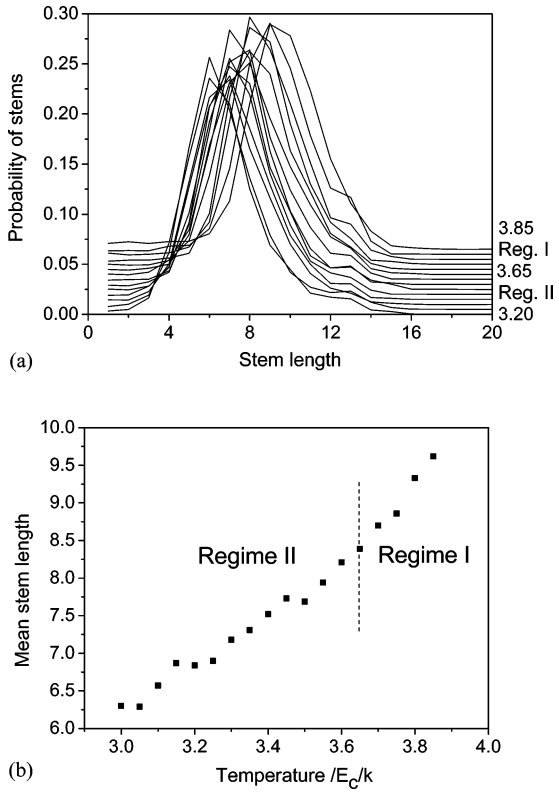

Figure 10. (a) Stem-length distributions and (b) mean stem lengths in the crystallites grown from the solution with polymer volume fraction 0.125 under variable temperatures. The stem length was defined as the number of consecutively connected crystalline bonds along the chain, each crystalline bond containing more than 15 parallel neighbors. In part a, the curves are drawn with equally spaced vertical offsets for clarity. In part b, the dashed line indicates a regime I−II transition.

again the experimental observations about the temperature dependence of crystal thickness.

We made visual inspections on the snapshots of crystallites obtained after crystal growth in the solutions. As shown in Figures 11a−d, deep coves can be easily observed at the crystal growth fronts in regime II; while in regime I the growth fronts become gently smooth with their horizontals indicating the crystalline registration for a facet of single crystals, although they are not so smooth as in a single crystalline layer. The roughness of the crystal growth front cannot be mapped with microfacets, which has been proposed to explain the round 200 facet of PE single crystals grown in regime I.[70,71] Therefore, the theoretical idea for single or multiple nucleation on a wide smooth crystal growth front is apparently not applicable in the present observations.

The deep coves at the crystal growth front may easily generate spiral dislocations upon lamellar crystal growth, especially when the stems are tilted in the single crystals with curvatures like tent- or chair-shapes, which have, indeed, been observed for crystal growth in regime II.[72] Such a growth instability in width is another conventional source of lamellar branching and splaying for spherulite formation at low temperatures, and be worthy of further studies in comparison with the growth instability in height as observed in Figure 5a,b.

The solution with the polymer volume fraction of 0.5 exhibits only a regime II−III transition at $T = 3.50$, where again, the multiple lamellar crystal growth starts to happen. If we selected the middle concentration at 0.25 between 0.5 and 0.125, both regime I−II and regime II−III transitions can be observed, as demonstrated in Figure 12. Regime II−III transition occurs exactly at $T = 3.20$ where multiple lamellae start to occur. The equilibrium melting point was selected at 5.40, which gave equal slopes in regime I and regime III but almost half in regime II, evidencing again the generality of intrinsic regime transitions for folded-chain crystal growth of polymers.

C. Chain Conformation in the Semicrystalline Texture. The adjacent-chain-folding model for polymer crystallization has been challenged by the switchboard model.[73] The latter considered that at low temperatures fast crystal growth in the bulk phase of interpenetrated random coils might not have enough time to make regular chain folding in the lamellar crystal.[73,74] However, if all the stems are connected to random coils without enough amount of immediate folding-back, there exists a serious overcrowding problem for those coils on the basal surfaces of polymer lamellar crystals.[75] MC simulations based on the random-walking model have suggested the least amount of adjacent chain folding to avoid the overcrowding problem.[76−78] Such a lower limit has been supposed to be reached in regime III, where the surface overcrowding gives rise to PE stems significantly tilted in the crystallites.[10] Therefore, the probability of adjacent chain folding in each regime is an interesting issue worth for an immediate addressing in the present study.

We defined the adjacent chain folding as the short loops (containing less than five monomers) connecting two different stems within the distance of next neighbors in the lamellar crystallites. Its probability was further defined as the ratio of the total amount of adjacent chain folding to the total amount of crystalline stems. The results for several sample systems are summarized in Figure 13. One can see that dilution makes a larger probability of adjacent chain folding. This observation is consistent with our common sense that perfect single crystals are grown more easily from dilute solutions than from the melt.[4,5] However, the probability of adjacent chain folding increases slightly with the decrease of temperatures and insensitive to the regime transitions. The high probability of chain folding at low temperatures is quite contradictory to the previous expectation for crystal growth at low temperatures,[10] albeit close to the high value proposed by Guttman et al.[79] to interpret the neutron scattering data.[80] We think that at the crystal growth front, the surface crystal nucleation may generate the adjacent chain folding with a probability increasing slightly with the increase of temperatures; during instant crystal thickening at the growth front, more adjacent chain folding will be sacrificed to make thicker crystals at higher temperatures, like in the case of decreasing integer number of chain folding for short-chain crystallization at high temperatures. Such a thickening may reverse the temperature dependence of the folding probabilities and thus explains the slightly higher probability of adjacent chain folding resulting at lower temperatures.

We also checked the crystallinity of those polymer chains joining crystal growth, which was defined as the fraction of crystalline bonds (presumably containing more than 15 parallel neighbors) in those polymers participating in the crystalline phase. The results for several sample systems are summarized in Figure 14. One can see that dilution makes a higher crystallinity of polymer chains participating in the crystallites, again in agreement with our common sense for the crystal growth from dilute solutions. The observed crystallinities appear insensitive to the regime transitions and decrease with the decrease of temperatures. The latter part of this result implies more amorphous fractions of polymers on the fold-end surface of lamellar crystals at lower temperatures. Therefore, for the melt crystallization at low temperatures, the richness of the noncrystalline parts of chains rather than the lack of adjacent

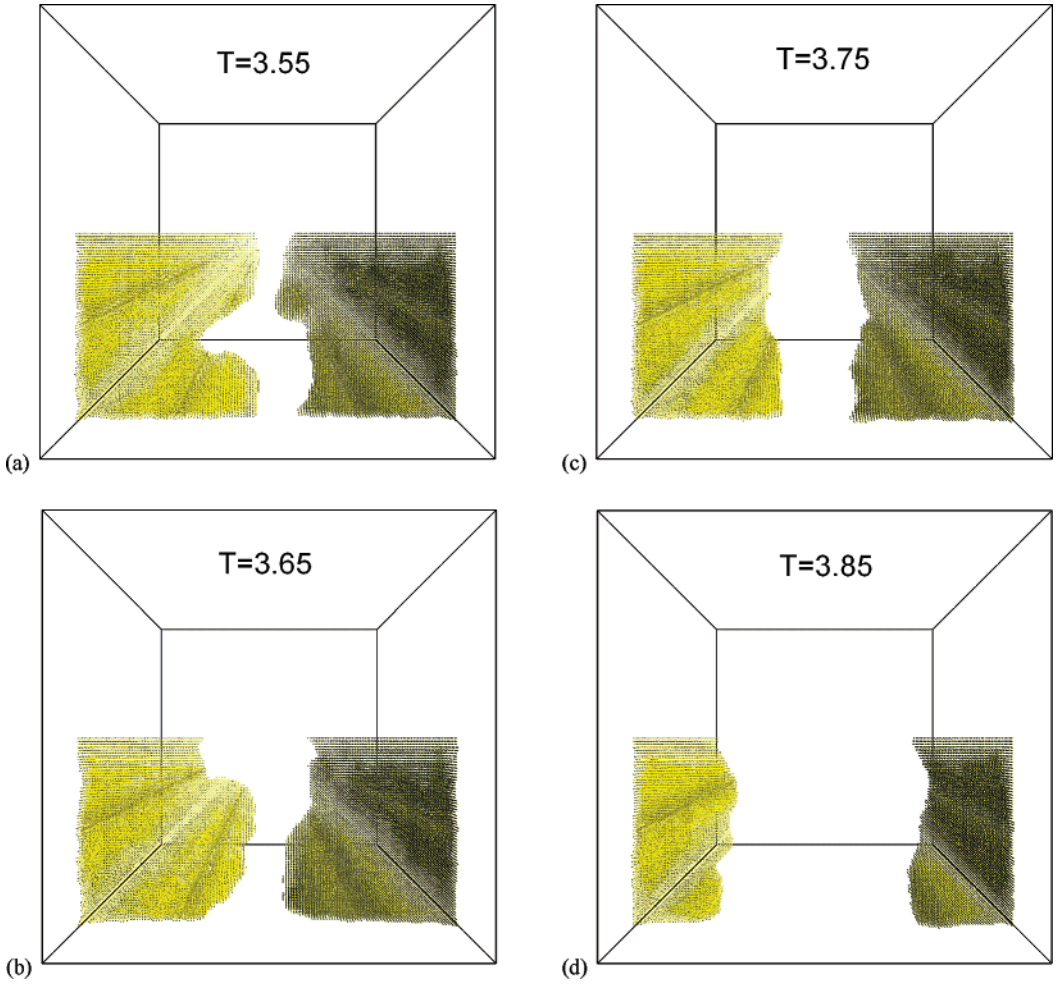

Figure 11. Snapshots of the crystal growth states at the temperatures (a) 3.55 in regime II, (b) 3.65 at regime I−II transition, (c) 3.75 in regime I, and (d) 3.85 in regime I after the periods of 3.91×10^5, 5.24×10^5, 1.04×10^6, and 1.60×10^6 MC cycles respectively for the solution samples (the volume fraction 0.125) containing a template of folded chains with folding lengths 16 at $X = 128$. The cubic box has a linear size 128, and the periodic boundary conditions occur at both $Y = Z = 64$ and $X = 128$. Only the bonds containing more than 15 parallel neighbors are drawn in tiny cylinders. All the figures are viewed along the *Z*-axis from the top of single lamella.

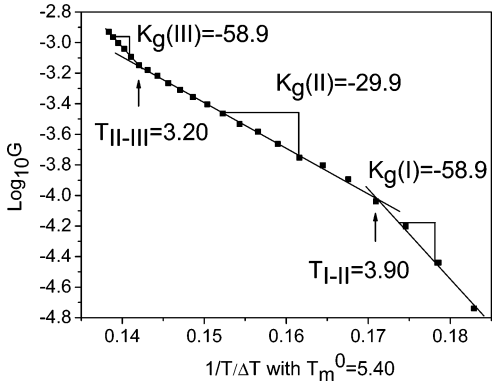

Figure 12. Logarithmic linear growth rates vs $(1/T)/\Delta T$ with $T_m^0 = 5.40$, showing three distinct regimes with the ratios of their slopes close to two in the solution with polymer volume fraction 0.25. The straight lines result from linear regression. The arrows indicate the transition temperatures at 3.20 and 3.90, respectively.

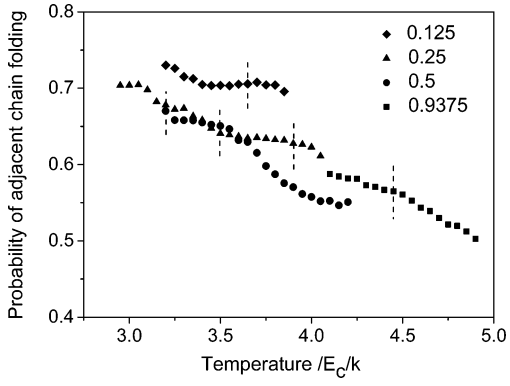

Figure 13. Probabilities of adjacent chain folding in the crystallites obtained from several polymer systems with denoted volume fractions under variable temperatures. For the definition of adjacent chain folding, see the text. Dashed short lines indicate the temperatures of regime transitions.

chain folding will be responsible for the experimentally observed surface overcrowding that leads to the tilting of PE stems in the crystallites.

The mean square radius of gyration of polymer chains can be measured by the neutron scattering experiments, which reflect the deviation of coil sizes from the initial melt state. Correspondingly, we calculated the average sizes of those polymers participating in the crystallites, and the results are summarized in Figure 15. One can see that dilution effectively decreases the coil sizes of semicrystalline polymers participating in the crystallites, implying more perfect chain folding in those solution-grown crystals. This observation is in consistence with the higher probability of adjacent chain folding and the higher crystallinity of those polymer chains participating in the crystallites upon dilution, as revealed in Figures 13 and 14. In solutions with the concentrations 0.125 and 0.25, the coil sizes

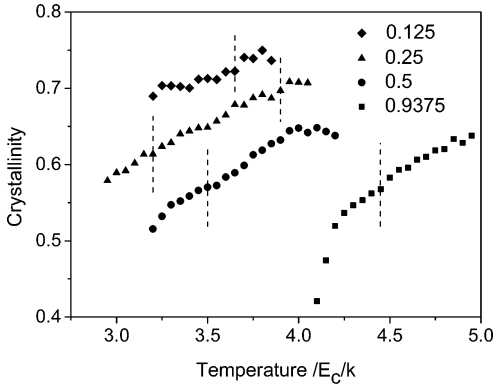

Figure 14. Crystallinities of those polymer chains participating in the crystallites obtained from several polymer systems with denoted volume fractions under variable temperatures. For the definition of the crystallinity, see the text. Dashed short lines indicate the temperatures of regime transitions.

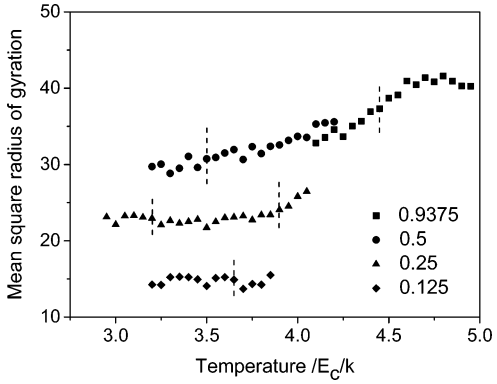

Figure 15. Mean square radius of gyration of those polymer chains participating in the crystallites obtained from several polymer systems with denoted volume fractions under variable temperatures. Dashed short lines indicate the temperatures of regime transitions.

appear insensitive to the temperatures and regime transitions. In the melt and the solution with the concentration 0.5, the coil sizes of semicrystalline polymers decrease down to the initial coil sizes (about 30) with the decrease of temperatures, especially in regime III of the bulk phase. This is because at high temperatures the stem lengths are larger than the initial coil sizes, and polymers become slightly stretched in the crystalline phase. With the decrease of temperatures, polymer coils have less and less time for a large-scale reorganization to adapt themselves into the fast advancing growth front at low temperatures, along with the decrease of average stem lengths. The extreme situation has been discussed under the cold crystallization by Wunderlich[81] and the *Erstarrungsmodell* (solidification model) by Fischer,[82] which provides a reasonable background for the proposition of the switchboard model.[73,74] The behavior naturally yields a lower crystallinity for melt crystallization at lower temperatures as revealed in Figure 14, but that does not mean a smaller probability of adjacent chain folding as revealed in Figure 13.

IV. Theoretical Interpretation

A. Consensus on Polymer Crystallization. As has been introduced at the beginning of this paper, the regime analysis rests on the general agreement that the lamellar crystal growth is dominated by the secondary crystal nucleation on a smooth crystal growth front, in company with the subsequent lateral spreading.[15−17,21,22,83] Such a consensus has been well adopted in the LH model.

In the LH model, the process of surface nucleation was assumed as putting the first stem with its length equal to the crystal thickness,[11,12] although later on, the idea was further patched with the assumption of a partial deposition in the first stem.[13,17] Point argued that the chain folding could happen even before the first stem has approached to the length of crystal thickness.[84,85] Frank and Tosi suggested the consideration of instant thickening at the crystal growth front.[69] The thickening growth of PE extended-chain crystals under a high pressure has already been observed by Wunderlich and his collaborators.[86,87] Hikosaka developed the LH model to consider both lateral spreading and thickening via sliding diffusion in two-dimensional crystal growth at the growth front.[88,89] Keller et. al further introduced the concept of mesophase at the wedge-shaped growth top of PE crystals under the consideration of the finite-size stability.[90] This idea was recently expanded into a general scheme by Strobl to explain the experimental data obtained in his group.[91,92] An apparent instant thickening at the crystal growth front is quite plausible, although the sliding diffusion may become very difficult inside the crystalline phase where the defects have been mostly removed. The snapshots shown in Figure 1b and Figure 5a,b clearly demonstrate the thickening process at the crystal growth front. Such an important process has, however, been missed in the LH model.

There are also existing converted points of view against the above consensus adopted by the LH model, among which the most representative model is the Sadler−Gilmer model,[93−95] or the so-called entropy-barrier model in order to be distinguished from the enthalpy-barrier model, for the LH model considers the nucleation barrier dominated by the surface free enthalpy.[7−9] The entropy-barrier approach proposed that the crystal growth is hindered by the pinning of ill-folded conformation at the crystal growth front. Another representative approach is the bundle model initiated by Allegra,[96] who proposed that the crystal growth of polymers was preformed by the bundles of prefolded crystalline clusters. The most recently updated model of this approach is the anisotropic aggregation model proposed by Zhang and Muthukumar.[97] For spherulite formation, phase-field simulations can reproduce various symmetric and asymmetric dendrites under the interplay of long-distance diffusion and crystal growth.[98] These approaches, although possibly worked well in the large-scale morphology of polymer crystal growth, disregarded the role of chain connection and the nucleation-controlled mechanism in the kinetics of polymer crystal growth. Therefore, they made no sense to the regime analysis that rested on the nucleation-controlled process (see eq 1) with chain folding. We have to leave them alone in the further discussions about regime transitions.

In the LH model, the assumption for a large-scale smooth crystal growth front is also arguable.[46−48] Neutron scattering experiments on the almost perfect single crystals grown from dilute solutions revealed the general existence of superfolding for polymers performing adjacent chain folding over several crystal growth layers.[99] This result implies that, right after the surface nucleation, lateral spreading may not be able to develop over the scope of single polymer. It was supposed that the impingement of surface nuclei generated long cilia, and the latter would start another event of surface nucleation on the next layer to form superfolding.[83,99] Such a cilium nucleation has been discussed by Sanchez and DiMarzio[100] for a dominant path of crystal growth and by Toda et. al[83] for the regime II crystal growth of long chains. Our simulations indeed demonstrate a rough surface for the crystal growth in regime I, as shown in Figure 11c,d. Therefore, for the surface nucleation on a smooth substrate, the width of the smooth substrate may never be requested beyond the scope of single polymers.

The intramolecular crystal nucleation as the dominant mode of surface nucleation can fit well into the above consensus. We proposed here a new interpretation of regime transitions on the basis of the intramolecular-crystal-nucleation model. A preliminary version of this idea has been presented recently at the 234th ACS National Meeting held in Boston, MA.[101]

B. Chain Folding via Intramolecular Crystal Nucleation. People are always curious to ask the question why so much adjacent chain folding can be generated to form the lamellar crystallites in the crystallization of flexible polymers. In principle, the fully extended chains earn the greatest enthalpy of the crystalline phase to stabilize the bulk phase at low temperatures. Considering the cold crystallization, the switchboard model, and the solidification model, chain folding is the most economic path toward a metastable crystalline phase without a large-scale reorganization from the initial melt. However, these models may not convince the assumption that a high percentage of adjacent chain folding can be restored from the initially interpenetrated random coils. So chain folding must be originated through an activation process and the appropriate candidate for such an activation process is the crystal nucleation. Polymer chains sequentially join into the crystalline phase at the crystal growth front according to their original locations in the amorphous phase. If we look at a single isolated chain performing crystallization, for example, the β-sheet formation upon protein folding, we will see that adjacent chain folding is a natural wisdom for the single chain to make the most parallel packing and meanwhile the least contacts with the surroundings at low temperatures. This wisdom implies that an intramolecular crystal nucleation via adjacent chain folding can effectively decrease the crystal nucleation barrier, and thus becomes the dominant kinetic path of polymer crystal nucleation.[4]

Intramolecular crystal nucleation means that both primary and secondary crystal nucleation are initiated by those monomers belonging to the same chains. Wunderlich and Mehta have proposed a speculative concept of molecular nucleation to address the crystal nucleation initiated by each new polymer.[4,102] This concept was recently developed into a theory of intramolecular crystal nucleation, evidenced by the simulations of single polymers performing intrachain crystallization.[103,104] In this theory, the classical nucleation theory has been applied to the isolated single-chain system. A body free energy gain and a surface free energy penalty constitute the total free energy change on crystal nucleation. For the secondary crystal nucleation, assuming the fully extended state of a single polymer buried inside the bulk crystalline phase as the ground state, the free energy change of the single polymer partially attached onto the crystal growth front is given by[103]

$$F = nf + s(N - n)^{1/2} \tag{2}$$

where n is the number of molten monomers, f is the free energy of fusion per monomer, s is the surface free energy density absorbing all the prefactors, and N is the chain length. According to this expression, the free energy barrier for secondary crystal nucleation becomes

$$F_c = s^2/(4f) \tag{3}$$

This result predicts two basic facts: the free energy barrier for crystal growth is of independence on the chain lengths and exhibits a linear relationship with the reciprocal of supercooling since f contains an approximately linear relationship with the supercooling.

The free energy expression also predicts an equilibrium melting point of two-dimensional single-chain single crystal (T_m^{2D}) for a specified chain length. In reverse, at each crystallization temperature, there exists a critical chain length (N_c) with its T_m^{2D} equal to the crystallization temperature, as given by

$$N_c = (s/f)^2 \tag{4}$$

For a polydisperse polymer sample, those chains with their lengths smaller than N_c will not be able to participate into crystal growth due to their T_m^{2D} lower than the crystallization temperature, and thus exhibit molecular segregation, as evidenced recently by molecular simulations.[54] On the other hand, T_m^{2D} is much lower than T_m^0. This feature explains why the initiation of polymer crystallization with chain folding always requires for a large supercooling. After each event of surface crystal nucleation, lateral spreading by feeding monomers along the chain is supposed to stop before reaching both chain ends, since many factors, such as the impingement of surface nuclei, the limited size of the crystal growth front, and the entanglement restriction for the diffusion along the chain, will prohibit further lateral spreading. Therefore, if the rest part of the chain at one chain end, often called as cilia, is longer than N_c at the crystal growth front, it will continue to perform another event of secondary crystal nucleation on the crystal growth front. It is imaginable that along each long chain several events of secondary crystal nucleation will be eventually generated either in the different positions of the same crystallites to form loops or in the different crystallites to form tie molecules, especially at low temperatures when N_c becomes much smaller. Such a picture can be well described by the variable-cluster model discussed by Hoffman.[22]

Note that the intramolecular crystal nucleation does not reject the existence of intermolecular crystal nucleation. There are many cases where the intermolecular crystal nucleation may dominate the crystallization process, such as for very short chains, for very rigid chains, for stretched chains, and in the polymerization process, etc. Adjacent chain folding is not a commonly favorite result in these cases.

C. New Interpretation of Regime Transitions. As illustrated in Figure 16a, we assume that on the crystal growth front, the intramolecular secondary crystal nucleation is initiated by the local slack part of the chain. The length of this slack part of the chain is denoted as S ($>N_c$), representing those monomers along the chain that can be activated to form the folded-chain crystallite on the crystal growth front. The surface crystal nucleation usually runs over the course not well designed, so the chain-folded nuclei may contain many defects and very limited fold lengths. An instant reorganization process including the crystal thickening and lateral spreading must follow the nucleation process. Further lateral spreading (also accompanied by crystal thickening) will pull the rest part of the chain from the amorphous surroundings, and this process requires for a long-distance diffusion along the polymer chain.

In regime I, the surface nucleation rate is so slow that lateral spreading has enough time to provide a wide new layer, and on the new layer the next event of surface nucleation can be hosted, as depicted in Figure 16b. So the advancing speed of the growth front is dominated by the rate of intramolecular secondary nucleation, as given by

$$1/t = ilL \tag{5}$$

where t is the incubation period for surface nucleation, l the lamellar thickness at the crystal growth front, L is the spreading

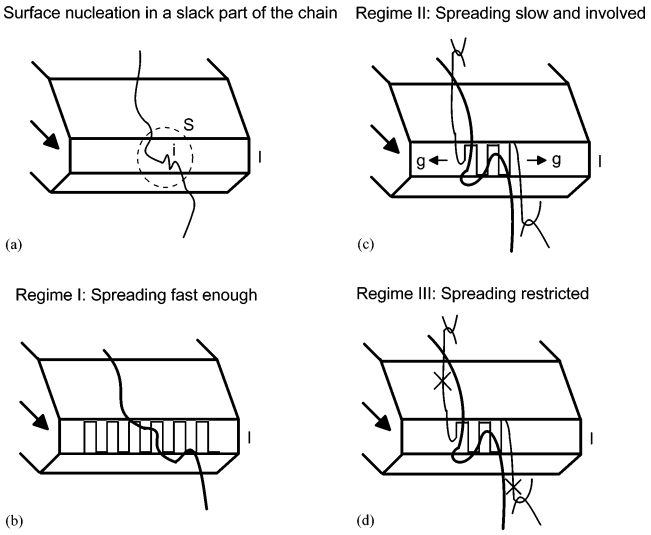

Figure 16. Depictions of intramolecular secondary crystal nucleation on the wedge-shaped growth front of a lamellar crystal. Key: (a) slack part of the chain performing surface nucleation; (b) regime I; (c) regime II; (d) regime III. The thick slack chain starts the next event of surface nucleation on the new substrate. *S* denotes the length of the slack part of the chain with the coil size marked by the dashed circle, *l* is the thickness of the growth front, *i* is the surface nucleation rate per area, and *g* is the spreading rate on the crystal growth front.

width of the smooth substrate, and *i* is the rate of secondary nucleation in the unit area of the substrate surface. The width of the smooth substrate required for an event of intramolecular nucleation in eq 5 can be estimated as the outreach range of the slack part of the chain, as given by

$$L \sim bS^{1/2} \tag{6}$$

where *b* is the linear size of a monomer. Here, the slack is assumed *a priori* random coil, so its linear size is about $bS^{1/2}$, insensitive to the temperature change. The previous assumption for a large-scale smooth substrate in the LH theory can thus be avoided. In addition, the fold ends, loops and cilia rather than the lateral surface of stems contribute dominantly the surface free energy barrier of nucleation, so the substrate may not be necessary to have a perfect crystalline smoothness even within the scope of the slack part of the chain, but shall have an enough thickness to accommodate the crystalline stems. Local steps of stems on the substrate are thus allowed at the crystal growth front in regime I, as observed in Figure 11c,d. Nevertheless, under the thermodynamic driving forces for perfect crystals with minimum surface tensions, the reorganization after nucleation and spreading intends to smoothen the growth front within the incubation period of the next event of surface nucleation. Therefore, there appears to be no deep cove at the crystal growth front of regime I.

In regime II, the surface nucleation rate becomes faster, and lateral spreading cannot catch up with the nucleation rate in the preparation of the new substrate layer, as illustrated in Figure 16c. The spreading rate thus interferes with the advancing speed of the crystal growth front. Labeling the lateral spreading rate on the crystal growth front as *g*, the width of a new layer to host the subsequent nucleation event is given by $L = 2gt$. So putting this *L* into eq 5, the advancing speed of the crystal growth front becomes

$$1/t = (2ilg)^{1/2} \tag{7}$$

The extent of enhancement of lateral spreading to meet the requirement of a fast nucleation is limited by the diffusion speed of long chains with the reptation mode in the entangled amorphous phase, as discussed by Hoffman and his coworkers.[10,41,42] In this sense, dilution helps the long-distance diffusion of polymer chains and thus enhances the lateral spreading more, so it will shift regime I−II transition to lower temperatures, as when comparing Figure 9 with Figure 12.

In regime III, the feeding for lateral spreading is completely restricted by some reasons, so the advancing of the crystal growth front has to be determined solely by the surface nucleation rate of the slack part of the chain on a width-restricted substrate, as depicted in Figure 16d. Following eq 5, we have

$$1/t = ilL' \tag{8}$$

where L' is the width of the substrate completely covered by the slack part of the chain and can be calculated as

$$L' \sim b^2S/l \tag{9}$$

Since the width-restricted substrate should be narrower than that in regime I, i.e., $L' < L$, otherwise the surface nucleation will not be influenced by the spreading, one can derive $l > bS^{1/2} > bN_c^{1/2} = bs/f$. This result implies that at low temperatures the substrate thickness to host the surface nucleation must be larger than a minimum value proportional to the reciprocal of supercooling. This minimum thickness will eventually evolve into the higher thickness of those mature crystallites measurable in the experiments. However, the details of this evolution process is still unclear, which possibly contains a mesophase transition as considered by Strobl.[92]

The reasons for restricting the feeding of monomers along the chain can be various. When two nearby lamellar crystals grow in parallel, tie molecules and dead entanglements in the amorphous region between two lamellae will frequently prohibit the feeding along the chain for further lateral spreading at the crystal growth front. This restriction will force the crystal growth to switch from regime II to regime III, and thus explains our simulation observations on regime II−III transition in company with the morphological transition from single to multiple lamellar crystal growth. The same restriction also exists in the subsequent crystal thickening for the saturate crystal thickness, as reflected by a small shift in the stem-length distributions in Figure 6a,b.

Such a restriction occurs only when two lamellae grow in parallel within a distance comparable with the coil sizes. The growth instability at low temperatures will eventually make the branching density of lamellar crystals reach this criterion, so the morphological trend of spherulites can be associated with regime II−III transition. In polymers with ultrahigh MW or a lightly cross-linked structure, the long-distance diffusion for lateral spreading will be prohibited by the dead entanglements and the cross-links in the space between nearby growing lamellae; therefore, only regime III behavior can be observed. In the case of ultrahigh MW, two lamellae growing in parallel will tighten up those tie molecules and interlocked loops in the amorphous region between them and thus deplete the slack part of the chain to prevent new crystals from growing in this region, although they may have a large distance but shall be within the scope of coil sizes. So with the increase of ultrahigh MW, the crystallinity significantly decreases and meanwhile the long spacing of lamellar crystals increases, as observed in the experiments.[105] Such a depletion prohibits the branching lamellae to fill into the amorphous space between these lamellae and thus be responsible for the irregular spherulites of ultrahigh MW PE.[10] In a heavily cross-linked structure of PE, regime II

restores.[40] This regime II behavior can be attributed to the noncrystalline cross-links (like comonomers) shortening the crystallizable sequences and then decreasing the nucleation rate, so the requested size in lateral spreading can be fulfilled by the slack part of the chain if the nucleation is not very fast, for example, low-density PE exhibits normally regime II behaviors.[6]

At high temperatures, the more extent of lateral spreading will yield the more adjacent chain folding on the crystal growth front. However, the crystal thickening behind the crystal growth front will eat some amount of adjacent chain folding. The thicker the mature crystallites approach, the more the adjacent chain folding loses. Therefore, we observed eventually a relatively high probability of adjacent chain folding in the mature crystallites at low temperatures, as revealed in Figure 13.

V. Concluding Remarks

In a summary of our observations, molecular simulations have evidenced the intrinsic regime I−II and II−III transitions in the temperature dependence of crystal growth rates of polymers. Regime II−III transition is raised with a morphological transition from branching to splaying of lamellar crystal growth, in parallel with the trend of spherulite formation from the sequential filling to the completed inner filling at low temperatures. Conformational analysis of the semicrystalline texture revealed that the surface overcrowding of PE lamellar crystals at low temperatures could be attributed to the richness of noncrystalline parts of the chain rather than the shortage of adjacent chain folding. On the other hand, regime I−II transition exhibits no large-scale smooth crystal growth front. We proposed a new interpretation of regime transitions for a better understanding of the experimental and simulation observations.

The LH model is only a specific model among the diverse points of view on the general mechanism of polymer crystallization, which has been criticized by several arguments on its interpretation of regime transitions. Our interpretation of regime transitions is based on the intramolecular-crystal-nucleation model that can be regarded as the source of adjacent chain folding for flexible polymers. The new interpretation of regime I−II transition shares the same basic scheme with the LH theory, albeit in a much smaller intramolecular scale. The new interpretation of regime II−III transition focuses on a complete restriction in the feeding of monomers along the chain for lateral spreading. Such a restriction may be originated by the parallel lamellar crystals growing within a distance comparable with coil sizes of polymers.

Here, we actually focus our attention only on the free energy barrier for secondary crystal nucleation of flexible polymers. The intramolecular crystal nucleation still contains many challenges for further studies. The properties of other terms in eq 1, such as the MW dependence of the prefactor G_0, the diffusion ability across interfaces, and the role of chain inflexibility, as well as the other processes following the crystal nucleation, such as the instant crystal thickening, the long-distance diffusion, and the crystal perfection, are calling for more extensive investigations and communications, in order to figure out a comprehensive picture on polymer crystallization behaviors.

Acknowledgment. W.H. thanks Bernhard Wunderlich, Stephen Z. D. Cheng, Gert Strobl, Bernard Lotz, Günter Reiter, Akihiko Toda, Jamie Hobbs, Paul J. Phillips, Andrew Lovinger, Murugapan Muthukumar, and Lei Zhu for helpful discussions. The financial support from the Chinese Ministry of Education (NCET-04-0448) and the National Natural Science Foundation of China (NSFC Grant Nos. 20474027, 20674036) is appreciated.

Supporting Information Available: Three movies showing the crystal growth from the melt induced by the template layer at $T = 4.40$, 4.45 and 4.50, respectively. Each frame was recorded in every 1000 MC cycles. Only those bonds containing more than 15 parallel neighbors are drawn as the crystalline bonds in tiny cylinders. This material is available free of charge via the Internet at http://pubs.acs.org.

References and Notes

(1) Keller, A. *Philos. Mag.* **1957**, *2*, 1171.
(2) Fischer, E. W. *Z. Naturforsch.* **1957**, *12a*, 753.
(3) Till, P. H., Jr. *J. Polym. Sci.* **1957**, *24*, 301.
(4) Wunderlich, B. *Macromolecular Physics, Vol. 2 Crystal Nucleation, Growth, Annealing*; Academic Press: New York, 1976; Chapter VI, p 115.
(5) Bassett, D. C. *Principles of polymer morphology*; Cambridge University Press: London, 1981; Chapter VI, p 146.
(6) Phillips, P. J. *Rep. Prog. Phys.* **1990**, *53*, 549.
(7) Armitstead, K.; Goldbeck-Wood, G. *Adv. Polym. Sci.* **1992**, *100*, 219.
(8) Gedde, U. W. *Polymer Physics*; Chapman and Hall: London, 1995; p 178.
(9) Cheng, S. Z. D; Lotz, B. *Polymer* **2005**, *46*, 8662.
(10) See the updated review of this theory: Hoffman, J. D.; Miller, R. L. *Polymer* **1997**, *38*, 3151.
(11) Lauritzen, J. I., Jr.; Hoffman, J. D. *J. Res. Natl. Bur. Stand.* **1960**, *64A*, 73.
(12) Hoffman, J. D.; Lauritzen, J. I., Jr. *J. Res. Natl. Bur. Stand.* **1961**, *65A*, 297.
(13) Hoffman, J. D.; Davis, J. T.; Lauritzen, J. I., Jr. In *Treatise on Solid State Chemistry*; Hannay, N. B., Ed.; Plenum: New York, 1976; Vol. 3; Chapter VII, p 497.
(14) Hillig, W. B. *Acta Metall.* **1966**, *14*, 1868.
(15) Frank, F. C. *J. Cryst. Growth* **1974**, *22*, 233.
(16) Sanchez, I. C.; DiMarzio, E. A. *J. Res. Nat. Bur. Stand.* **1972**, *76A*, 213.
(17) Lauritzen, J. I., Jr.; Hoffman, J. D. *J. Appl. Phys.* **1973**, *44*, 4340.
(18) Lauritzen, J. I., Jr. *J. Appl. Phys.* **1973**, *44*, 4353.
(19) Pelzbauer, Z.; Galeski, A. *J. Polym. Sci., Part C: Polym. Symp.* **1972**, *38*, 23.
(20) Barham, P. J.; Jarvis, D. A.; Keller, A. *J. Polym. Sci., Part B: Polym. Phys.* **1982**, *20*, 1733.
(21) Phillips, P. J. *Polym. Prep. (Am. Chem. Soc., Polym. Chem. Div.)* **1979**, *20*, 438.
(22) Hoffman, J. D. *Polymer* **1983**, *24*, 3.
(23) Armistead, J. P.; Hoffman, J. D. *Macromolecules* **2002**, *35*, 3895.
(24) Cheng, S. Z. D.; Janimak, J. J.; Zhang, A.-Q.; Cheng, H. N. *Macromolecules* **1990**, *23*, 298.
(25) Cheng, S. Z. D.; Chen, J.; Janimak, J. J. *Polymer* **1990**, *31*, 1018.
(26) Lovinger, A. J.; Davis, D. D.; Padden, F. J., Jr. *Polymer* **1985**, *26*, 1595.
(27) Phillips, P. J.; Vatansever, N. *Macromolecules* **1987**, *20*, 2138.
(28) Lazcano, S.; Fatou, J. G.; Marco, C.; Bello, A. *Polymer* **1988**, *29*, 2076.
(29) Hoffman, J. D.; Frolen, L. J.; Ross, G. S.; Lauritzen, J. I., Jr. *J. Res. Nat. Bur. Stand.* **1975**, *79A*, 671.
(30) Vasanthakumari, R.; Pennings, A. J. *Polymer* **1983**, *24*, 175.
(31) Roitman, D. B.; Marand, H.; Miller, R. L.; Hoffman, J. D. *J. Phys. Chem.* **1989**, *93*, 6919.
(32) Toda, A. *Colloid Polym. Sci.* **1992**, *270*, 667.
(33) Organ, S. J.; Keller, A. *J. Polym. Sci., Part B: Polym. Phys.* **1986**, *24*, 2319.
(34) Allen, R. C.; Mandelkern, L. *Polym. Bull. (Berlin)* **1987**, *17*, 473.
(35) Toda, A. *Polymer* **1987**, *28*, 1645.
(36) Hoffman, J. D. *Macromolecules* **1986**, *19*, 1124.
(37) Hoffman, J. D. *Polymer* **1991**, *32*, 2828.
(38) Ungar, G. *Adv. Polym. Sci.* **2005**, *180*, 45.
(39) Ergos, F.; Fatou, J. G.; Mandelkern, L. *Macromolecules* **1972**, *5*, 147.
(40) Phillips, P. J.; Lambert, W. S. *Macromolecules* **1990**, *23*, 2075.
(41) Hoffman, J. D. *Polymer* **1982**, *23*, 656.
(42) Hoffman, J. D.; Miller, M. L. *Macromolecules* **1988**, *21*, 3038.
(43) Hoffman, J. D. *Polymer* **1985**, *26*, 803.
(44) Hoffman, J. D. *Polymer* **1985**, *26*, 1763.
(45) Hoffman, J. D.; Miller, M. L. *Macromolecules* **1989**, *22*, 3502.
(46) Dosiere, M.; Colet, M. C.; Point, J. J. *J. Polym. Sci.; Polym. Phys. Ed.* **1986**, *24*, 345.
(47) Point, J. J.; Colet, M. C.; Dosiere, M. *J. Polym. Sci.; Polym. Phys. Ed.* **1986**, *24*, 357.
(48) Point, J. J.; Dosiere, M. *Macromolecules* **1989**, *22*, 3501.
(49) Point, J. J. *Macromolecules* **1997**, *30*, 1375.
(50) Kovacs, A. J.; Straupe, C. *Faraday Dicuss. Chem. Soc.* **1979**, *68*, 225.

(51) Cheng, S. Z. D.; Chen, J.; Barley, J. S.; Zhang, A.; Habenschuss, A.; Zschack, P. R. *Macromolecules* **1992**, *25*, 1453.
(52) Janimak, J. J.; Cheng, S. Z. D.; Jiusti, P. A.; Hsieh, E. T. *Macromolecules* **1992**, *24*, 2253.
(53) Hu, W.-B.; Frenkel, D. *Adv. Polym. Sci.* **2005**, *191*, 1. See the Appendix for more details of simulation techniques.
(54) Hu, W.-B. *Macromolecules* **2005**, *38*, 8712.
(55) Yamamoto, T. *J. Chem. Phys.* **1997**, *107*, 2653.
(56) Waheed, N.; Lavine, M. S.; Rutledge, G. C. *J. Chem. Phys.* **2002**, *116*, 2301.
(57) Gee, R. H.; Lacevic, N.; Fried, L. E. *Nat. Mater.* **2006**, *5*, 39.
(58) Kreer, T.; Baschnagel, J.; Mueller, M.; Binder, K. *Macromolecules* **2001**, *34*, 1105.
(59) Hu, W.-B. *J. Chem. Phys.* **1998**, *109*, 3686.
(60) Hu, W.-B. *J. Chem. Phys.* **2000**, *113*, 3901.
(61) Hu, W.-B. *J. Chem. Phys.* **2001**, *115*, 4395.
(62) Hu, W.-B.; Mathot, V. B. F. *J. Chem. Phys.* **2003**, *119*, 10953.
(63) Zha, L.-Y.; Hu, W.-B. *J. Phys. Chem. B* **2007**, *111*, 11373.
(64) Hoffman, J. D. *J. Chem. Phys.* **1958**, *29*, 1192.
(65) Hoffman, J. D.; Weeks, J. J. *J. Chem. Phys.* **1962**, *37*, 1723.
(66) Strobl, G. *The Physics of Polymers*, 3rd ed.; Springer-Verlag: Berlin and Heidelberg, Germany, 2007; p 184.
(67) Lotz, B.; Cheng, S. Z. D. *Polymer* **2005**, *46*, 577.
(68) Bassett, D. C.; Olley, R. H. *Polymer* **1984**, *25*, 935.
(69) Frank, F. C.; Tosi, M. *Proc. R. Soc. London* **1961**, *A263*, 323.
(70) Mansfield, M. L. *Polymer* **1988**, *29*, 1755.
(71) Hoffman, J. D.; Miller, M. L. *Macromolecules* **1989**, *22*, 3038.
(72) Toda, A.; Okamura, M.; Hikosaka, M.; Nakagawa, M. *Polymer* **2005**, *46*, 8708.
(73) Flory, P. J. *J. Am. Chem. Soc.* **1962**, *84*, 2857.
(74) Flory, P. J.; Yoon, D. Y. *Nature* (*London*) **1978**, *272*, 226.
(75) Frank, F. C. *Faraday Discuss. Chem. Soc.* **1979**, *68*, 7.
(76) Guttman, C. M.; DiMarzio, E. A.; Hoffman, J. D. *Polymer* **1981**, *22*, 1466.
(77) Guttman, C. M.; DiMarzio, E. A. *Macromolecules* **1982**, *15*, 525.
(78) Mansfield, M. L. *Macromolecules* **1983**, *16*, 914.
(79) Guttman, C. M.; Hoffman, J. D.; Dimarzio, E. A. *Faraday Discuss. Chem. Soc.* **1979**, *68*, 297.
(80) Schelten, J.; Ballard, D. G. H.; Wignall, G. D.; Longman, G.; Schmaltz, W. *Polymer* **1976**, *17*, 751.
(81) Wunderlich, B. *J. Chem. Phys.* **1958**, *29*, 1395.
(82) Fisher, E. W. *Pure Appl. Chem.* **1978**, *50*, 1319.
(83) Toda, A.; Kiho, H.; Miyaji, H.; Asai, K. *J. Phys. Soc. Jpn.* **1985**, *54*, 1411.
(84) Point, J. J. *Macromolecules* **1979**,.
(85) Point, J. J. *Faraday Discuss. Chem. Soc.* **1979**, *68*, 297.
(86) Wunderlich, B.; Melillo, L. *Makromol. Chem.* **1968**, *118*, 250.
(87) Wunderlich, B.; Davidson, T. *J. Polym. Sci., Part A2* **1969**, *7*, 2043.
(88) Hikosaka, M. *Polymer* **1987**, *28*, 1257.
(89) Hikosaka, M. *Polymer* **1990**, *31*, 458.
(90) Keller, A.; Hikosaka, M.; Rastogi, S.; Toda, A.; Barham, P. J.; Goldbeck-Wood, G. *J. Mater. Sci.* **1994**, *29*, 2579.
(91) Strobl, G. *Eur. Phys. J. E.* **2005**, *18*, 295.
(92) Strobl, G. *Prog. Polym. Sci.* **2006**, *31*, 398.
(93) Sadler, D. M.; Gilmer, G. H. *Polymer* **1984**, *25*, 1446.
(94) Sadler, D. M.; Gilmer, G. H. *Phys. Rev. Lett.* **1986**, *56*, 2708.
(95) Sadler, D. M. *Nature (London)* **1987**, *326*, 174.
(96) Allegra, G. *Ferroelectrics* **1980**, *30*, 195.
(97) Zhang, J.; Muthukumar, M. *J. Chem. Phys.* **2007**, *126*, 234904.
(98) Granasy, L.; Pusztai, T.; Borzsonyi, T.; Warren, J. A.; Douglas, J. F. *Nat. Mater.* **2004**, *3*, 645.
(99) Sadler, D. M.; Keller, A. *Science* **1979**, *203*, 263.
(100) Sanchez, I. C.; DiMarzio, E. A. *J. Chem. Phys.* **1971**, *55*, 893.
(101) Hu, W.-B. *ACS PMSE Prepr.* **2007**, *97*, 811.
(102) Wunderlich, B.; Mehta, A. *J. Polym. Sci., Part B: Polym. Phys.* **1974**, *12*, 255.
(103) Hu, W.-B.; Frenkel, D.; Mathot, V. B. F. *Macromolecules* **2003**, *36*, 8178.
(104) Hu, W.-B. In Lecture Notes in Physics 714. *Progress in Understanding of Polymer Crystallization*; Reiter, G., Strobl, G., Eds.; Springer-Verlag: Berlin and Heidelberg, Germany, 2007; p 47.
(105) Robelin-Souffache, E.; Rault, J. *Macromolecules* **1989**, *22*, 3581.

MA702636G